ISME

www.nature.com/ismej

ARTICLE

Chemotaxis may assist marine heterotrophic bacterial diazotrophs to find microzones suitable for N_2 fixation in the pelagic ocean

Søren Hallstrøm[1], Jean-Baptiste Raina[2], Martin Ostrowski[2], Donovan H. Parks[3], Gene W. Tyson[4], Philip Hugenholtz[3], Roman Stocker[5], Justin R. Seymour[2] and Lasse Riemann[1]✉

Heterotrophic bacterial diazotrophs (HBDs) are ubiquitous in the pelagic ocean, where they have been predicted to carry out the anaerobic process of nitrogen fixation within low-oxygen microenvironments associated with marine pelagic particles. However, the mechanisms enabling particle colonization by HBDs are unknown. We hypothesized that HBDs use chemotaxis to locate and colonize suitable microenvironments, and showed that a cultivated marine HBD is chemotactic toward amino acids and phytoplankton-derived DOM. Using an in situ chemotaxis assay, we also discovered that diverse HBDs at a coastal site are motile and chemotactic toward DOM from various phytoplankton taxa and, indeed, that the proportion of diazotrophs was up to seven times higher among the motile fraction of the bacterial community compared to the bulk seawater community. Finally, three of four HBD isolates and 16 of 17 HBD metagenome assembled genomes, recovered from major ocean basins and locations along the Australian coast, each encoded >85% of proteins affiliated with the bacterial chemotaxis pathway. These results document the widespread capacity for chemotaxis in diverse and globally relevant marine HBDs. We suggest that HBDs could use chemotaxis to seek out and colonize low-oxygen microenvironments suitable for nitrogen fixation, such as those formed on marine particles. Chemotaxis in HBDs could therefore affect marine nitrogen and carbon biogeochemistry by facilitating nitrogen fixation within otherwise oxic waters, while also altering particle degradation and the efficiency of the biological pump.

The ISME Journal (2022) 16:2525–2534; https://doi.org/10.1038/s41396-022-01299-4

INTRODUCTION

Dinitrogen (N_2) fixation, the biological conversion of N_2 gas to ammonium (NH_4^+), is performed exclusively by specific bacteria and archaea, collectively termed diazotrophs. In tropical and subtropical oligotrophic oceanic regions, where bioavailable nitrogen often limits primary production, N_2 fixation is an ecologically important process influencing nitrogen (N) and carbon (C) biogeochemistry [1, 2]. During the last decade, the known biogeography of marine N_2 fixation has expanded, with recent reports of considerable N_2 fixation in coastal, deep sea, temperate, and Arctic environments [3–8]. Furthermore, recent work has revealed the overlooked diversity of marine diazotrophs. While cyanobacteria were long thought to be the only relevant N_2 fixing organisms in marine systems (reviewed in [9]), it is now recognized that phylogenetically diverse heterotrophic bacterial diazotrophs (HBDs) are widespread and active in the global ocean [10–13]. However, the ecology of HBDs and their significance for nitrogen cycling in marine environments remains poorly understood [14, 15].

N_2 fixation is an anaerobic process [16], whereby oxygen irreversibly inhibits the nitrogenase enzyme [17]. Diazotrophic cyanobacteria overcome the limiting effects of oxygen by applying either a physical or temporal separation of N_2 fixation and oxygenic phototrophy [18]. However, given that cellular protection from oxygen is energetically costly [19], evidence for N_2 fixation by HBDs in oxygenated ocean waters [7, 15] is somewhat paradoxical. It has been hypothesized that HBDs may be able to perform nitrogen fixation in oxic waters by colonizing low-oxygen microenvironments associated with marine particles [20, 21].

The potential for particles to be suitable loci for N_2 fixation by HBDs has gained recent support [22] based on observations of HBDs attached to particulate matter [23–27], experimental evidence of efficient surface colonization by HBDs [28, 29], stimulated N_2 fixation in response to particle addition [28, 30], and trait-based modeling of the mechanisms enabling bacteria proliferate and N_2 fixation on sinking particles [31]. However, a prerequisite for this idea would be that HBDs are motile and chemotactic (able to direct movements according to chemical gradients). Some heterotrophic marine bacteria exhibit chemotactic responses of high sensitivity and precision [32–36], with chemotactic behavior facilitating bacterial exploitation of even ephemeral microscale nutrient patches [32]. For instance, organic

[1]Marine Biological Section, Department of Biology, University of Copenhagen, Helsingør, Denmark. [2]Climate Change Cluster, Faculty of Science, University of Technology Sydney, Sydney, NSW, Australia. [3]Australian Centre for Ecogenomics, School of Chemistry and Molecular Biosciences, The University of Queensland, St. Lucia, QLD, Australia. [4]Centre for Microbiome Research, School of Biomedical Science, Translational Research Institute, Queensland University of Technology, Woolloongabba, QLD, Australia. [5]Institute of Environmental Engineering, Department of Civil, Environmental and Geomatic Engineering, ETH Zurich, Zurich, Switzerland. ✉email: lriemann@bio.ku.dk

Received: 14 February 2022 Revised: 18 July 2022 Accepted: 20 July 2022
Published online: 1 August 2022

solutes, such as amino acids [37] and phytoplankton-derived dissolved organic matter (DOM) [38] can form concentration gradients [39, 40] that may guide motile bacteria through chemotaxis [41]. Indeed, a broad range of prokaryotes in marine bacterioplankton has the capacity to sense and respond to microscale patches of phytoplankton-derived DOM [42], yet whether HBDs are generally motile and use chemotaxis is unknown.

In this study, we hypothesized that motility and chemotaxis are widespread among HBDs in the marine environment. To test this, we employed a novel microfluidic platform [43, 44] to directly quantify chemotactic behavior toward amino acids and phytoplankton-derived organic materials in both HBD isolates and putative HBDs in a natural bacterioplankton community in situ. Metagenomes derived from these in situ measurements revealed the diversity and phylogeny of the motile and chemotactic HBDs. Finally, we surveyed genomes of HBD isolates, obtained from the Baltic Sea and the Pacific Ocean, and metagenome assembled genomes (MAGs) recovered from the *Tara* Oceans global sampling campaign [12] and the Australian Microbiome Initiative (AMI, https://www.australianmicrobiome.com/), for the presence of genes related to motility and chemotaxis. Using these distinct approaches, we build a case for chemotaxis being a widespread and important functional trait in HBDs.

MATERIALS AND METHODS

Laboratory chemotaxis experiments with bacterial isolates

The HBDs, *Pseudomonas stutzeri* BAL361, *Raoultella ornitinolytica* BAL286 (Gammaproteobacteria), and *Rhodopseudomonas palustris* BAL398 (Alphaproteobacteria), isolated from the Baltic Sea [45, 46], were grown at room temperature in ZoBell broth adjusted to salinity 8 [47] and screened for motility by observing cells using an Eclipse Ci microscope equipped with phase contrast (Nikon, Tokyo, Japan).

Two HBD isolates, *P. stutzeri* and *R. palustris*, exhibited motility and were subsequently prepared for laboratory chemotaxis experiments as follows. Overnight cultures of *P. stutzeri* and *R. palustris* ($OD_{600} = 0.6$ (1 day) and $OD_{600} = 0.3$ (2 day), respectively) were diluted 1:1000 in 1% ZoBell broth (in phosphate-buffered saline (PBS); autoclaved; salinity 8; pH 7.4; Medicago, Uppsala, Sweden), incubated for an additional 2 h, before being diluted 10-fold in PBS to obtain a cell suspension of ~$1–2 \times 10^6$ cells ml^{-1}.

To investigate the chemotactic capabilities of HBD isolates in laboratory experiments, as well as natural assemblages of HBDs in the marine environment, we used the in situ chemotaxis assay (ISCA; [43, 44]). This microfluidic device is composed of an array of wells linked to the outside environment by a port (Fig. S1A). Putative chemoattractants are loaded into the wells and, following ISCA deployment, diffuse out of the wells creating concentration gradients that are analogous to naturally occurring chemical hotspots. Motile and chemotactic cells can use these concentration gradients to migrate into the wells where they can then be sampled. All experiments were conducted with four ISCAs deployed in parallel ($n = 4$), with each ISCA allowing five technical replicates of five different treatments to be deployed simultaneously (Fig. S1B).

Chemotaxis experiments were performed with organic and inorganic N sources (glutamine, glutamate, cysteine, and NH_4^+; all at 1 mM) and phytoplankton-derived DOM (see below). Amino acids and phytoplankton-derived organic materials were chosen as chemoattractants because amino acids are released via ectoenzymatic hydrolysis of particles [39] and dead phytoplankton are an important constituent of marine particles [48–51], suggesting that gradients of these chemicals will emanate from particles [40]. Both isolates were tested with nitrogen sources, whereas only *P. stutzeri* was tested with phytoplankton-derived DOM (see below for additional information).

Phytoplankton-derived DOM was obtained from algal cells and exudates. For laboratory experiments, phytoplankton cultures of 200 ml (*Chlamydomonas reinhardtii* and *Thalassiosira pseudonana* CCMP 1335) were grown to stationary phase at their optimal light, temperature, and nutrient conditions. Cells were harvested by centrifugation ($1500 \times g$ for 10 min) and the pellet was snap frozen in liquid nitrogen for chemical extraction. The supernatant was filtered through a 0.2 µm filter and subjected to a solid-phase extraction (SPE) using Oasis HLB SPE columns (Waters Corp, Milford, MA, USA) following a protocol adapted from Dittmar et al. [52]. Briefly, supernatant was acidified to pH 2 using 10% HCl, and exuded metabolites were adsorbed onto the SPE cartridges using gravity flow. SPE cartridges were then dried for 20 min before being eluted with 75% HPLC-grade methanol, which was aliquoted and dried before use in chemotaxis assays. Phytoplankton-derived DOM was prepared by extracting organic matter from the pellet according to Raina et al. [42]. Briefly, cells were extracted with 75% HPLC-grade methanol, sonicated on ice to break the cell walls, and centrifuged at 13,000 rpm for 10 min to pellet the cell debris. Extracts were aliquoted, dried and normalized to 1 mg ml^{-1} before use in chemotaxis assays. Total organic carbon (TOC) in the phytoplankton extracts and exudates of *C. reinhardtii* and *T. pseudonana* used in the laboratory chemotaxis assays was measured on a TOC-L TOC analyzer (Shimadzu Corporation, Kyoto, Japan). Ultrafiltered PBS was used as control for the chemotaxis assay as well as to resuspend the different treatments and was prepared by sequential filtration through a 0.2 µm Millex FG filter (Millipore, Temecula, CA, USA), twice through a 0.2 µm Sterivex filter (Millipore), and through a 0.02 µm Anotop filter (Whatman, Kent, UK).

For laboratory-based chemotaxis experiments, ISCAs were secured inside sterile plastic trays and 1 h incubations at room temperature were initiated by the addition of 80 ml cell suspension [44]. Following incubations (see below), the contents of the ISCA wells were collected using a 1 ml syringe and a 27G needle (Terumo, Sydney, Australia). For each ISCA, the contents of five wells were pooled to gain ~550 µl, which was fixed with 0.2 µm-filtered glutaraldehyde (2% final concentration) for subsequent flow cytometry analysis (performed on the same day).

Samples for flow cytometry were stained with SYBR Green (1:10,000 final dilution; Thermo Fisher), incubated for 15 min in the dark and analyzed on a CytoFLEX (model LX and S) flow cytometer (Beckman Coulter, Brea, CA, USA) with filtered MilliQ water as sheath fluid. For each sample, forward scatter (FSC), side scatter (SSC), and green (SYBR) fluorescence were recorded and the samples were analyzed at a flow rate of 25 µl min^{-1}. Microbial populations were characterized according to SSC and SYBR Green fluorescence [53]. To quantify the strength of chemotaxis, the chemotactic index *Ic* was calculated by dividing the number of cells present in a given treatment by the average number of cells present in the control [43]. Thus, *Ic* values >1 indicate an attraction, while *Ic* values <1 suggest a repulsion.

Field deployment of the in situ chemotaxis assay (ISCA)

Field deployments of the ISCA were carried out on the 1st of February 2018 at Clovelly Beach (33.91°S, 151.26°E), a coastal location near Sydney, Australia, and additional results derived from this deployments are reported in Raina et al. [42]. Seawater freshly collected from the field site was ultrafiltered (as above) and used as a control and to resuspend the dried phytoplankton-derived organic matter (concentration: 1 mg ml^{-1}). Flow cytometry (as above) confirmed that the filtration protocol removed all bacterial cells from seawater.

Prior to the field deployment, phytoplankton cultures were grown to mid-exponential phase at their optimal light, temperature and nutrient conditions [42]. The supernatant was discarded, phytoplankton-derived DOM was extracted from the pellet (as above), and used as chemoattractant. Each phytoplankton-derived DOM treatment was resuspended in ultrafiltered seawater from the site at a concentration of 1 mg ml^{-1} and replicated across four ISCAs deployed simultaneously. Each ISCA was secured inside a sealed enclosure [43] and deployed at 1 m depth for 1 h. Upon retrieval, the contents of the ISCA wells were collected as described above with the following modification: from the pooled sample, 80 µl was fixed with 0.2 µm-filtered glutaraldehyde (2% final concentration) for flow cytometry analysis (conducted the same day) and 470 µl was snap-frozen in liquid nitrogen for subsequent DNA extraction. Bulk seawater samples (500 µl, $n = 4$) from the site (1 m depth) were also collected for flow cytometry and DNA sequencing.

DNA extraction from ISCA samples was performed under a UV clean hood (UVC/T-M-AR, Biosan, Riga, Latvia) using a microvolume physical lysis extraction [54]. Libraries for shotgun metagenome sequencing were prepared using the Nextera XT DNA Sample Preparation Kit (Illumina, San Diego, CA, USA) following a protocol designed for generating low-input DNA libraries [55]. All libraries were sequenced with an NextSeq 500 platform (Illumina) 2 × with 150 bp High Output v.2 run chemistry. Libraries were pooled on a shared sequencing run, resulting in 1/37 of a run or ~3 Gbp per sample.

Reads were processed using Trimmomatic v0.36 [56] to remove adapters, filter leading or trailing bases with a quality score <3, clip reads

when the average 4-base window had a quality score <15, and discard reads <50 bp in length. Read pairs passing QC were further processed to remove potential human contamination or contamination from phytoplankton strains used to produce DOM [42]. Specifically, paired reads were mapped to reference genomes or available transcriptomic data using the MEM mapping method of BWA v 0.7.12-r1039 [57] and pairs were discarded if either read had ≥95% identity and ≥95% alignment length to any reference genome.

Reads assigned to the *nifH* gene were identified following the functional annotation outlined in Raina et al. [42]. Briefly, a reference database was constructed from all UniRef100 [58] proteins available on 6th March 2018, which had a Kyoto Encyclopedia of Genes and Genomes (KEGG) Orthology (KO) annotation in the KEGG database [59]. Quality-controlled reads were compared to this reference database using the BLASTX option of DIAMOND v0.9.22 [60]. A read was assigned to a UniRef protein if the top hit had an *E*-value $<1e^{-3}$, a percent identity >30%, an alignment covering >70% of the read, and the UniRef100 protein was annotated as being bacterial or archaeal. Otherwise, the read was considered unclassified. Assigned reads were mapped to KO IDs using the UniProt ID mapping files. Hits to each KO were summed across all assigned reads to produce a KO count table for each sample.

Phylogenetic analysis of reads assigned to nifH

For all samples, paired-end reads of four biological replicates were analyzed. Taxonomic classification of reads assigned as *nifH* (K02588) was performed with GraftM (https://github.com/geronimp/graftM) using the precompiled NifH package (available at https://data.ace.uq.edu.au/public/graftm/7/). Ordination and cluster analysis was performed in the PRIMER + PERMANOVA software package (v6; [61]).

To determine whether the metagenomic reads were related to specific diazotrophic taxa, a further phylogenetic characterization was carried out using metagenomic *nifH* reads (≥100 bps, 6350 reads in total). A reference tree based on 138 *nifH* gene sequences from diverse reference genomes (selected from an initial set of 6040 reference sequences), including prominent environmental sequences, was constructed. Sequences were aligned using MAFFT (v. 7, [62]) and the reference tree was built with RAxML-NG [63] using the RAxML GUI 2.0 beta [64]. The metagenomic reads were placed onto the reference tree using EPA-ng [65] and a tree visualizing the phylogenetic placement was generated with the Gappa command-line toolkit [66].

The prevalence of chemotaxis and motility genes in marine HBDs

To explore the prevalence of chemotactic capacity among marine HBDs, genes related to chemotaxis and motility were surveyed in MAGs from the AMI (https://www.australianmicrobiome.com/) and *Tara* Oceans (https://www.embl.de/tara/). The HBD MAGs retrieved from the AMI database were recovered from several sampling sites in Australian coastal and open ocean waters, while the Tara Oceans HBD MAGs originate from the Pacific, Atlantic, and Indian Oceans([12]; Supplementary Information 2). MAGs retrieved from AMI database were surveyed for the presence of *nifH* using BLAST (https://blast.ncbi.nlm.nih.gov/Blast.cgi) and a curated *nifH* database (https://www.jzehrlab.com/nifh). Taxonomic assignments were obtained using the Genome Taxonomy Database Toolkit [67]. Additionally, genomes of four marine HBD isolates were included in the analysis. Three of these, *Pseudomonas stutzeri* BAL361, *Raoultella ornitinolytica* BAL286, and *Rhodopseudomonas palustris* BAL398 [68], were included in the experimental part of our study. In addition, alphaproteobacterium *Sagitulla castanea* P11, which was recently isolated off the coast of Chile and is genomically similar to sequences recovered from the South China Sea and the Indian Ocean ([69]; Supplementary Information 2), was included in the analysis.

MAGs and HBD isolate genomes were surveyed for the presence of 26 protein coding genes assigned to the KEGG pathway for bacterial chemotaxis (ko02030) using custom hidden Markov models (HMMs). Seed proteins used to build the custom HMMs were downloaded from UniProt (January 2020; https://www.uniprot.org/) and aligned using MAFFT (v. 7). HMMs were generated using hmmbuild from the HMMER toolbox (v. 3.2 (June 2018); http://hmmer.org/) with default settings. Prediction of open reading frames was performed with Prodigal v. 2.6.3 [70]. The predicted proteins were surveyed by the custom HMMs using hmmsearch with default settings. Trusted cutoffs (TCs) for the custom HMMs were determined by searching the seed proteins with the corresponding HMM and setting the cutoff to the lowest score. The resulting TC for methyl-accepting chemotaxis protein (Mcp) set by this approach was 8.9, i.e., not reliable, and a TC of 1×10^{-9} was used as for the Pfam Mcp domain. The TC for maltose binding protein (MalE) and methyl-accepting chemotaxis protein IV (Tap; 2.6×10^{-53} and 3.1×10^{-206}, respectively) were increased to 1×10^{-50} to improve their sensitivity (see Supplementary Table S1 for full list of TC values).

Statistical analyses

Statistical analysis was performed in R-4.0.0. All sample comparisons were carried out as follows: a Shapiro–Wilk's test was performed to test for normality using the R function "shapiro.test". A linear model was fitted using the function "lm" (stats v. 4.0.3) and the model statistics retrieved through a one-sided analysis of variance (ANOVA) using the function "anova" (car v. 3.0.10). For the comparison among groups, a post hoc test was performed using the function "emmeans" (emmeans v. 1.7.3). All data were transformed ($\log(x+1)$) prior to statistical analysis to meet the assumptions of the statistical tests. The output of the statistical tests can be found in Table S3.

RESULTS

Laboratory chemotaxis assays using diazotrophic bacterial isolates

Pseudomonas stutzeri exhibited significant chemotactic responses toward the three amino acids tested (ANOVA, $p < 0.05$; Fig. 1A). Specifically, glutamine, glutamate, and cysteine elicited a chemotactic index (*Ic*) of 2.41 ± 0.35 (SE), 2.14 ± 0.50, and 2.14 ± 0.11, respectively. The other motile HBD isolate tested, *Rhodopseudomonas palustris*, did not show a chemotactic response toward any of the amino acids (Fig. S2). Neither of the isolates exhibited positive chemotaxis toward NH_4^+. *P. stutzeri* also exhibited significant levels of chemotaxis toward DOM derived from the phytoplankton species *Chlamydomonas reinhardtii* and *Thalassiosira pseudonana* (Fig. 1B), with both cell extracts and exudates (supernatant) eliciting chemotactic responses. The *Chlamydomonas* exudates induced the greatest response, resulting in an *Ic* value of 14.26 ± 2.56 (ANOVA, $p < 0.001$). The *Chlamydomonas* cell extract elicited a chemotactic response with an *Ic* value of 6.70 ± 0.63 (ANOVA, $p < 0.001$). Both *Thalassiosira* cell extracts and exudates also produced positive chemotaxis, with *Ic* values of 3.70 ± 0.18 (ANOVA, $p < 0.001$) and 2.14 ± 0.31 (ANOVA, $p < 0.05$), respectively. The positive control used for these experiments (10% ZoBell broth) also elicited positive chemotaxis, with an *Ic* value of 2.30 ± 0.27 (ANOVA, $p < 0.05$). Notably, the level of chemotaxis was significantly higher for both *Chlamydomonas* treatments (ANOVA, $p < 0.001$) and the *Thalassiosira* pellet extract (ANOVA, $p < 0.05$) than was observed for the positive control. When normalizing cell counts to the amount of carbon in each phytoplankton treatment, we found that the *Chlamydomonas* exudate attracted 1750 ± 1000 cells more per nmol C than the *Chlamydomonas* cell extract (Fig. S3; ANOVA, $p < 0.05$). The normalization also showed that per nmol C there was no significant difference between the *Chlamydomonas* and *Thalassiosira* treatments. Taken together, these results show that the HBD *P. stutzeri* is capable of strong chemotaxis and indicate that phytoplankton-derived DOM elicits a larger chemotactic response than glutamine, glutamate, cysteine, and the rich 10% ZoBell medium.

Field deployment of the in situ chemotaxis assay (ISCA)

To assess the prevalence of chemotaxis among natural communities of diazotrophs, we deployed the ISCA with phytoplankton-derived DOM at a coastal location near Sydney, Australia. Natural microbial communities exhibited significant chemotaxis toward eight of the ten phytoplankton-derived DOM treatments relative to the filtered seawater (FSW) control (Fig. 2A). The strongest response was induced by *Alexandrium*-derived DOM, which elicited an *Ic* value of 4.85 ± 0.70 (ANOVA, $p < 0.001$), *Prymnesium*-derived DOM resulted in an *Ic* of 3.66 ± 0.99 (ANOVA, $p < 0.01$), whereas the *Dunaliella* and *Thalassiosira*-derived DOM

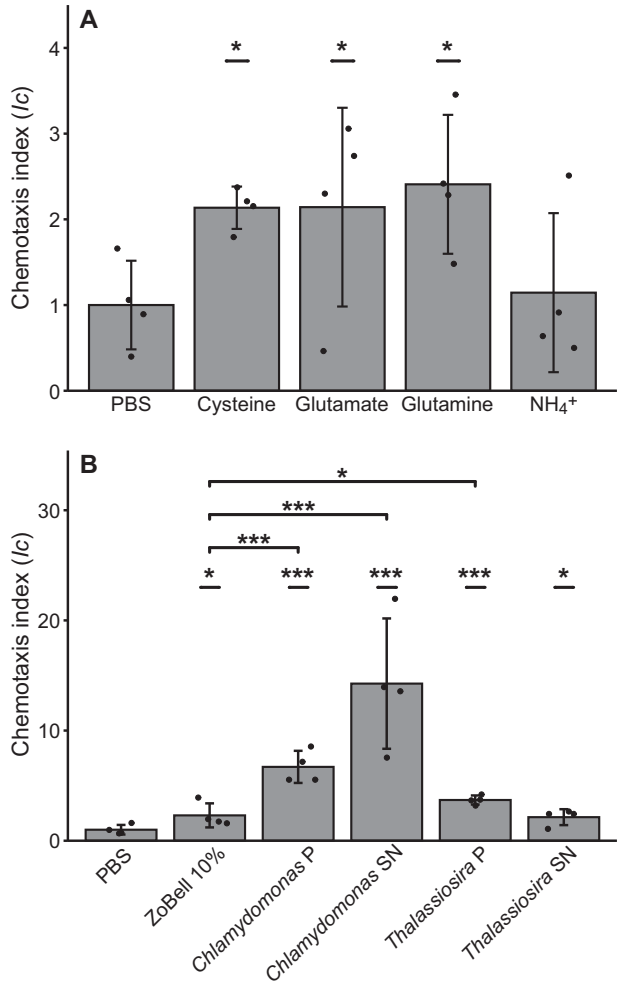

Fig. 1 Chemotaxis by *Pseudomonas stutzeri*. Chemotaxis index (*Ic*) of *P. stutzeri* exposed to **A** 1 mM concentrations of amino acids and NH_4^+ and **B** 1 mg ml^{-1} cell extracts (pellet (P)) and exudates (supernatant (SN)) of cultured *Chlamydomonas reinhardtii* (green algae) and *Thalassiosira pseudonana* (diatom). Treatments significantly different from control (phosphate-buffered saline, PBS) and positive control (10% ZoBell broth) are indicated (*$p < 0.05$, **$p < 0.01$, ***$p < 0.001$; $n = 4$; ANOVA (one-sided)). Error bars represent standard deviation.

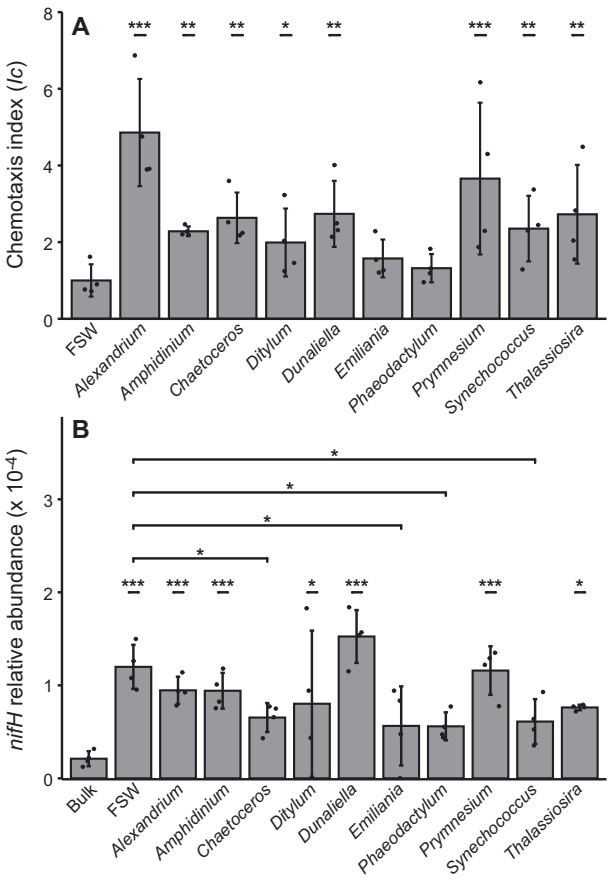

Fig. 2 Diazotrophs in a natural bacterioplankton community are motile and capable of performing chemotaxis. A Chemotaxis index calculated for each of the treatments. **B** The relative abundance of metagenomic reads mapping to *nifH* as a fraction of the total reads in each sample. Bulk (Bulk seawater), FSW (Filtered seawater); significance levels for differences between Bulk and FSW and treatments are indicated (*$p < 0.05$, **$p < 0.01$, ***$p < 0.001$; $n = 4$; ANOVA (one-sided)). Error bars represent standard deviation. **A** is a reproduction of data published in [42].

generated *Ic* values of 2.73 ± 0.43 (ANOVA, $p < 0.01$) and 2.72 ± 0.64 (ANOVA, $p < 0.05$), respectively [42]. For seven of the ten treatments, metagenomes derived from the ISCA wells revealed that reads mapping to *nifH* were significantly more abundant in the prokaryotic assemblages that entered the ISCA wells, which selects for motile and chemotactic cells, compared to bulk seawater (Fig. 2B; ANOVA; $p < 0.001$). Specifically, the relative abundance of reads mapping to *nifH* were 7 ± 4 times higher in the FSW treatment (which selects for motile though not necessarily chemotactic cells) compared to bulk seawater. This indicates that the motile fraction of the bacterial community contained a significantly higher proportion of diazotrophs than the bulk community.

We sought to determine whether HBDs were specifically attracted to the phytoplankton-derived DOM. The chemotactic populations from six of the ten DOM treatments had similar *nifH* abundances to FSW, whereas four treatments had significantly lower *nifH* abundances (Fig. 2B). However, the *Ic* values of the phytoplankton-derived DOM treatments ranged between 1.9 and 4.9 (i.e., the treatments that elicited a significant chemotactic response attracted on average 2.6 ± 1.0 times more cells than the FSW control). In order to quantify the difference in response between each treatment and the FSW control, the normalized cell counts (*Ic* values) were multiplied by the relative abundance of *nifH*. This normalization of chemotactic responses to metagenomic reads assigned to *nifH* indicated that three of the ten treatments (*Alexandrium, Dunaliella*, and *Prymnesium*) had higher responses compared to FSW (Fig. S4; ANOVA, $p < 0.05$). This indicates that *nifH* containing cells were enriched in the three phytoplankton treatments compared to the FSW—i.e., motile diazotrophs were attracted to these three phytoplankton treatments.

Diversity of *nifH* sequences recovered from the field deployment

The metagenomic reads mapping to *nifH* (average 132 nt; range 61–151 nt) were analyzed to gain insight into the composition of the diazotrophs that entered the ISCA wells. Taxonomic assignment by GraftM using the precompiled NifH package enabled classification of 46% of the metagenomic *nifH* sequences (Table S2) and revealed a diverse community of motile diazotrophs dominated by HBDs (Fig. 3). Calculation of the Shannon index of alpha diversity showed that six of the ten phytoplankton treatments attracted a higher diversity of diazotrophs than FSW (Fig. 3A; ANOVA, $p < 0.01$). Principal coordinate analysis of Bray-Curtis similarity revealed that the diazotroph communities in four

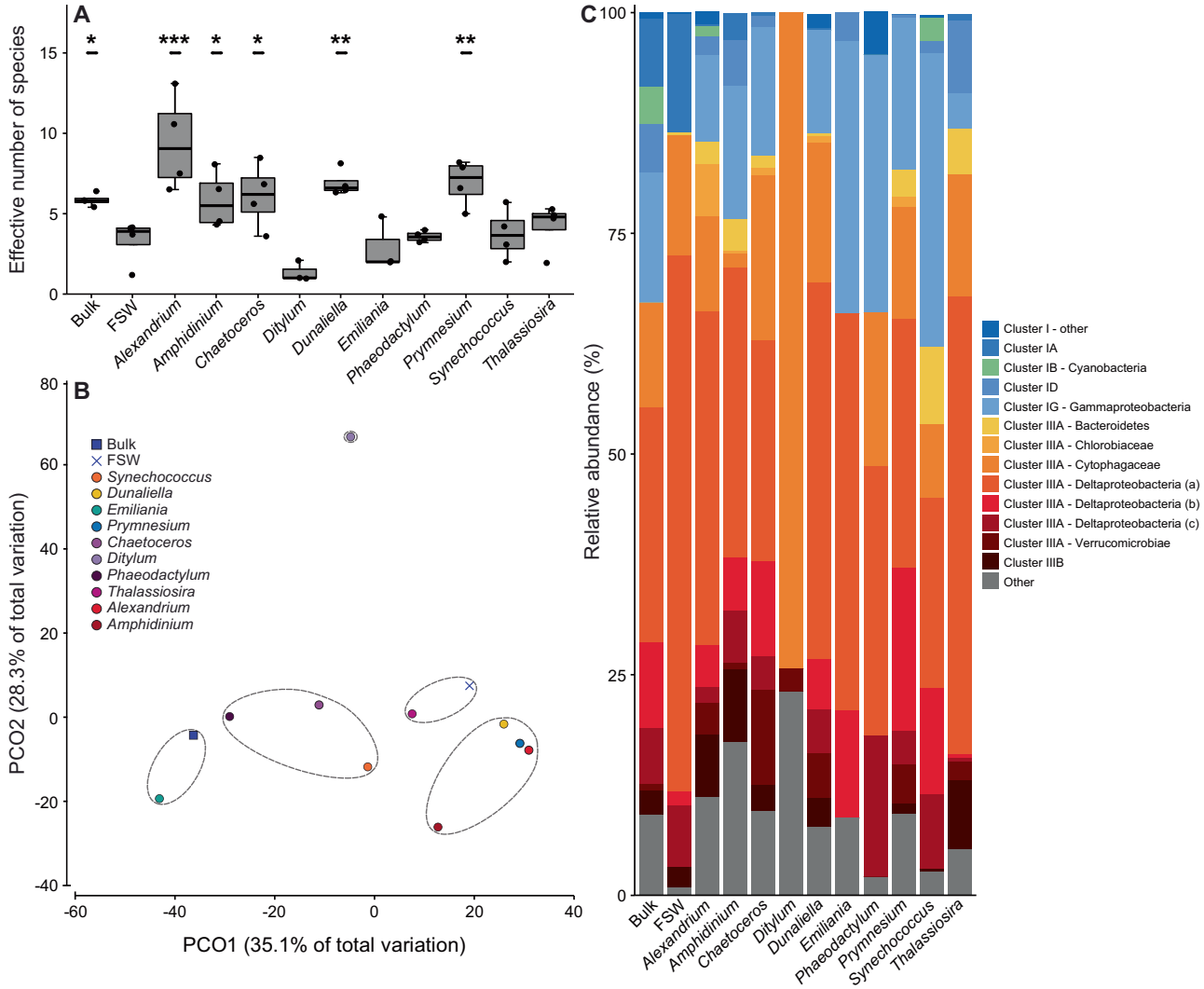

Fig. 3 Diversity and composition of motile and chemotactic diazotrophs. Analysis of metagenomic reads assigned as *nifH* obtained from the In situ chemotaxis assay. **A** Boxplot showing the range and median of the effective number of species calculated for each independent sample replicate. Significance levels reported in **A** is the difference between FSW and Bulk seawater and phytoplankton treatments (**$p < 0.01$; ***$p < 0.001$; $n = 4$; ANOVA (one-sided)). **B** Principal coordinate analysis (PCO) of Bray-Curtis similarity. Bulk (Bulk seawater), FSW (Filtered seawater); dotted line represents 60% similarity. **C** The relative abundance of classified metagenomic reads assigned as *nifH* combined for the four biological replicates. Blues: Cluster I, Green: Cluster I Cyanobacteria, Yellow, reds, and black: Cluster III, and Gray: Others. **B**, **C** are based on averaged relative abundances of four biological replicates.

of the six treatments that attracted a significantly higher diversity of diazotrophs, namely the *Alexandrium*, *Amphidinium, Dunaliella*, and *Prymnesium* treatments, exhibiting chemotaxis toward these three phytoplankton treatments clustered at 55% similarity (Fig. 3B). The diazotroph communities in the FSW and the *Thalassiosira* treatments clustered together, while bulk seawater communities clustered with the *Emiliania* treatment.

Of the classified reads, 96% were annotated as *nifH* Cluster I and Cluster III sequences (Fig. 3C), with the great majority being HBDs. Of all sequences, only 4% in bulk seawater, 3% in *Synechococcus* treatment, and 1% in the *Alexandrium* treatment were annotated as Cyanobacteria. The main *nifH*-harboring groups in bulk seawater samples were affiliated with Deltaproteobacteria (43%, including *Desulfobacteraceae* (10%) and *Desulfovibrionaceae* (6%)) and Bacteroidetes (*Cytophagaceae* (12%)) within Cluster III, and Gammaproteobacteria (15%) within Cluster I. The FSW control and the phytoplankton treatments contained on average 47 ± 7% Deltaproteobacteria, 17 ± 9% *Cytophagaceae*, and 15 ± 11% Cluster I Gammaproteobacteria. Bacteroidetes and Verrucomicrobia were not identified in either the bulk seawater or FSW control, but were detected in the phytoplankton treatments with average relative abundances of 3 ± 2% and 3 ± 3%, respectively. In summary, 33% and 59% of sequences annotated from the bulk seawater were assigned to Clusters I and III, respectively. In contrast, the average abundances in FSW and phytoplankton treatments were 20 ± 4% and 71 ± 7% for Clusters I and III, respectively, showing that Cluster III accounted for a larger pool of motile diazotrophs than Cluster I.

In order to investigate whether the metagenomic reads were related to environmental sequences of common diazotrophic taxa, reads (≥100 bases) were placed on a reference phylogenetic tree constructed of diverse *nifH* sequences including representatives of predominant environmental taxa (Supplemental Fig. S5; a full non-collapsed tree is available online; see Data availability section). The metagenomic reads of both the bulk seawater and the ISCA treatments were affiliated with reference sequences of *nifH* Clusters I and III, all of which belonged to HBDs. Most of the reads were affiliated with well-known diazotrophs, such as *Vibrio*

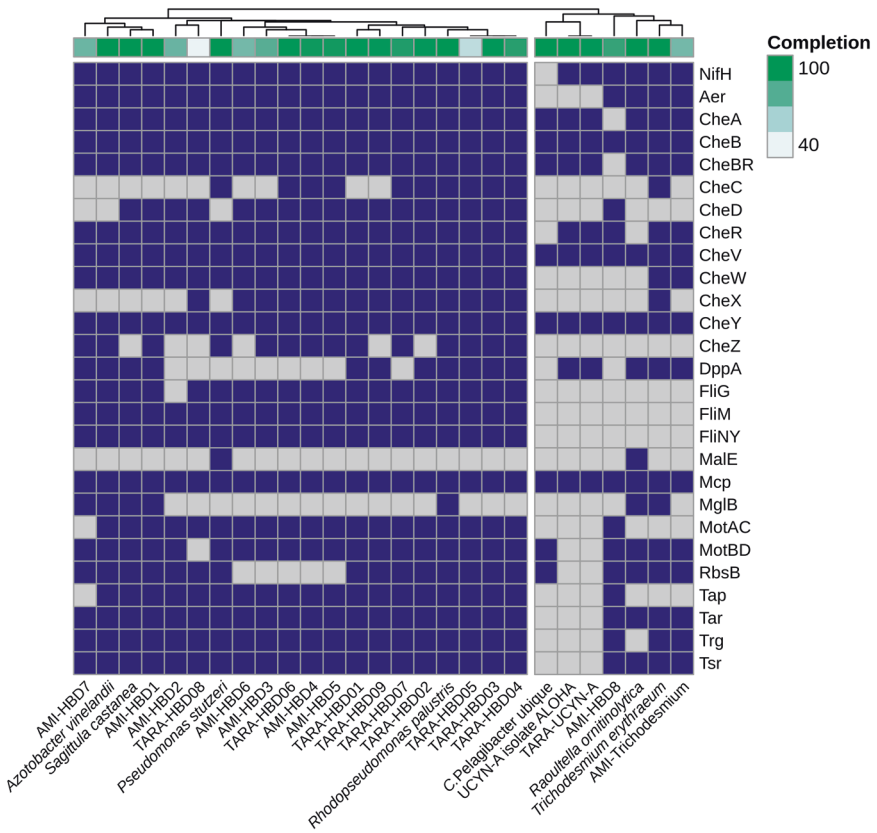

Fig. 4 Chemotaxis is a prevailing phenotype in HBDs. The presence (blue squares) or absence (gray squares) of genes assigned to the KEGG pathway for chemotaxis (ko02030) in four marine heterotrophic bacterial diazotroph (HBD) isolates, metagenome assembled genomes (MAGs) of 17 putative HBDs and two cyanobacterial diazotrophs from *Tara* oceans and AMI, and reference genomes of *Trichodesmium erythraeum*, UCYN-A, *Candidatus* Pelagibacter ubique (SAR11), and *Azotobacter vinelandii*. The genomes and MAGs are clustered based on the proteins present. See Supplementary Information 2 for detailed information of the MAGs, isolates, and reference genomes. Levels of completeness of genomes and MAGs are indicated above the chart.

Table 1. Summary of the genetic potential for motility and chemotaxis in the analyzed metagenome assembled genomes (MAGs) and genomes of cultivated heterotrophic bacterial diazotrophs (HBDs).

MAG collection or isolate collection	MAGs or isolates in the collection	Containing *nifH*	HBDs in collection	HBDs containing *che*, *fli*, and *mot* genes
Tara Oceans	957	10	9	9
AMI	741	9	8	7
Marine HBDs	4	4	4	3

See "Materials and methods" for references.
nifH nitrogenase reductase Fe-Subunit, *che* proteins involved in various stages of cellular chemotaxis such as the sensing of chemoattractants, intracellular signal transduction and transcriptional regulation, *fli* proteins involved in flagellar assembly, *mot* motor proteins involved in flagellar movement.

sp. and *Geobacter* sp. in Cluster I, and the Deltaproteobacteria *Desulfovibrio* sp., *Desulfuromonas* sp., and *Desulfobacter* sp. in Cluster III. These analyses confirmed that the majority of the *nifH* reads belonged to HBD taxa that are known to be motile [71–73].

Genetic survey of motility and chemotaxis

In order to determine if motility and chemotaxis are commonly associated with HBDs in the global ocean, we surveyed genomes of HBD isolates and MAGs derived from the *Tara* Oceans [12] and AMI metagenomes (https://www.australianmicrobiome.com) for the prevalence of core genes assigned to the KEGG pathway for bacterial flagellar chemotaxis (ko02030, Fig. 4). We considered a MAG or an isolate to be motile and chemotactic if the genome encoded flagellar proteins FliNY, FliM and FliG, motor proteins MotAC and MotBD, and >70% complete clusters of chemotaxis genes (CheA–CheZ) (Table 1). We surveyed four marine HBD isolates (including two Gammaproteobacteria (*P. stutzeri* and *Raoultella ornitinolytica*) and two Alphaproteobacteria (*R. palustris* and *Sagittula castanea* P11; [68, 69]) and 19 diazotroph MAGs (including 17 HBD MAGs and two cyanobacterial MAGs, originating from the *Tara* Oceans and AMI sampling campaigns, that were selected based on the presence of *nifH*). All of the *Tara* Oceans HBD MAGs and 7 of 8 AMI HBD MAGs met the criteria outlined above and were considered motile and chemotactic. In line with the experimental findings, *P. stutzeri* and *R. palustris* contained 88% and 100% of the genes encoding motility and chemotaxis, respectively, whereas only a fraction of these (37%) were present in the *R. ornitinolytica* genome. To further validate our approach, we included genomes of the non-motile nitrogen-fixing cyanobacteria *Candidatus* Atelocyanobacterium thalassa isolate ALOHA

(UCYN-A) and *Trichodesmium erythraeum* IMS101, as well as the non-nitrogen-fixing and non-motile *Candidatus* Pelagibacter ubique HTCC1062 (representative of the SAR11 clade) in our analysis. As expected, these organisms lack flagellar proteins and contain only parts of the chemotaxis and sensory pathways (Fig. 4). A cluster analysis based on the proteins present divided the isolates and MAGs into a motile and a non-motile group (Fig. 4). The motile group consisted of multiple subgroups, including two clusters dominated by Alphaproteobacteria, multiple groups comprised of Deltaproteobacteria, Gammaproteobacteria, and Planctomycetes, and finally, the *Oceanospirillaceae* MAGs, TARA-HBD03-05, that form a branch including the alphaproteobacterial HBD isolate *R. palustris*. The non-motile group consisted of UCYN-A and *T. erythraeum* reference genomes, clustering closely together with the respective cyanobacterial TARA-UCYN-A and AMI-Trichodesmium MAGs, as well as the non-motile HBD *R. ornithinolytica* and the non-nitrogen-fixing and non-motile *C.* Pelagibacter ubique. The AMI-HBD8 MAG, annotated as a proteobacterium, was also present in the non-motile group. All of the examined diazotroph genomes and MAGs, except for UCYN-A, harbored an aerotaxis receptor (Aer), enabling sensing of oxygen gradients [74].

DISCUSSION

HBDs are ubiquitous in oxic marine waters [11]. The suggestion that particles are suitable loci for heterotrophic N_2 fixation was recently revisited to rationalize the widespread distribution of diverse putative HBDs [10, 14, 22]. Since chemotaxis greatly increases the encounter rate with particles, we hypothesized that the capacity for chemotaxis is widespread among HBDs.

The HBD isolate *P. stutzeri* exhibited a chemotactic response to cysteine, glutamate, and glutamine, as well as phytoplankton-derived DOM from both the green alga *C. reinhardtii* and the diatom *T. pseudonana*. The finding that, per nmol C, the exudates of *C. reinhardtii* yielded higher cell counts than the cell extract indicates an enrichment of chemoattractants in the exudates of this green alga. Taken together, we show that *P. stutzeri* is attracted to both amino acids and phytoplankton-derived DOM, which potentially resembles the types of compounds emanating from organic particles in pelagic waters.

The field deployment of the ISCA revealed the capacity for motility and chemotaxis by a natural assemblage of HBDs in a coastal environment. The relative abundance of *nifH* in the metagenomes revealed up to 7-fold enrichment of HBDs in the FSW control treatment compared to the bulk seawater within which the ISCA was deployed. This indicates that HBDs are more prevalent among the motile pool of marine bacteria than among the overall bacterioplankton community. To evaluate differences in chemotaxis between the FSW control and the phytoplankton treatments, the changes in chemotactic response provided by the *Ic* values were normalized to the relative abundance of *nifH* genes. There are potential caveats associated with this normalization. For example, differences in gene copy number per genome between treatments could bias the comparability and the *Ic* values are calculated from a pool of bacteria of which the HBDs make up a small proportion. However, since the four replicates of FSW control and phytoplankton treatments were simultaneously deployed (thus exposed to the same bacterioplankton community), and subjected to the same processing and genetic analyses, we assume that the comparison was not affected by any directional or stochastic bias. The results of the normalization suggested chemotaxis by HBDs toward three treatments, *Alexandrium*, *Dunaliella*, and *Prymnesium*. Chemotaxis toward phytoplankton-derived DOM of three different types of algae that are widespread in marine and coastal environments, golden and green algae (*Prymnesium* and *Dunaliella*, respectively) and dinoflagellates (*Alexandrium*), suggest that attraction of HBDs to chemical cues of phytoplankton origin is a widespread phenomenon. Taken together, this first in situ measurement of the chemotactic behavior of HBDs suggests that diazotrophy is more prevalent among motile bacteria than in the overall bacterioplankton community, indicating that motile HBDs exhibit chemotaxis toward organic matter of phytoplankton origin.

The classification of metagenomic reads assigned as *nifH* showed that motile and chemotactic diazotrophs mainly belonged to Gammaproteobacteria in *nifH* Cluster I and Deltaproteobacteria in *nifH* Cluster III. A further phylogenetic characterization was conducted using metagenomics reads ≥100 bp to determine the relationship to common diazotrophic taxa by phylogenetic placement. This confirmed the predominance of Cluster I and Cluster III sequences. Reads were affiliated with *Vibrio* sp. and *Geobacter* sp. in Cluster I and Deltaproteobacterial sulfur bacteria in Cluster III. These diazotrophs are known from both marine and estuarine locations (e.g., [4, 5, 11]). Overall, the composition and high diversity of HBDs is consistent with *nifH* gene amplicon studies of bulk bacterioplankton from other coastal localities [4, 5, 8].

The high prevalence of chemotaxis among HBDs suggested by the in situ chemotaxis experiment was supported by our in silico survey of marine metagenomes and genomes of HBD isolates. Our HBD genome survey showed that 90% of HBD genomes (including 3 of 4 isolates and 16 of 17 HBD MAGs) harbor genes encoding motility and chemotaxis capabilities. These MAGs and HBD genomes represent diverse groups of bacteria, including Alpha-, Delta-, and Gammaproteobacteria, and Planctomycetes, and overlap largely with the groups identified in our ISCA. The analysis included isolates relevant in a global context and MAGs recovered from marine environments across the Australian maritime zone and from major ocean basins. In addition, the nine *Tara* Oceans HBD MAGs collectively have high in situ abundances, $0.5–3 \times 10^6$ cells l^{-1} [12]. Hence, our analysis provides a strong indication of chemotaxis being a general trait among HBDs in global marine bacterioplankton.

The survey of motility and chemotaxis in HBD isolates and MAGs suggested capability for sensing and responding to numerous chemical signals by harboring multiple substrate-binding proteins (e.g., MalE MglB, DppA) and specific sensory receptors for peptides, amino acids, and sugars (e.g., Tap, Tar, Trg, and Tsr). This allows chemotactic bacteria to sense and move along environmental gradients [75]—an ability that is critical for efficient navigation in the complex chemical microenvironments of marine particles [76]. However, not all examined HBDs encode the full array of auxiliary proteins, with some proteins found exclusively in subsets of the investigated HBDs. For instance, the three Alphaproteobacteria, *R. palustris, S. castanea*, and AMI-HBD7, and the Deltaproteobacteria AMI-HBD1 exclusively encode the methyl-galactoside binding protein MglB. Another example is the dipeptide substrate-binding protein DppA that is present in the same three Alphaproteobacteria, as well as three Deltaproteobacteria MAGS, AMI-HBD1 and HBD01 and HBD02 from *Tara* Oceans, and the *Oceanospirillaceae* (TARA-HBD03-05). All MAGs of *Pseudomonadales*, AMI-HBD3, TARA-HBD06, and TARA-HBD07, and *P. stutzeri* lack both of these proteins. Additionally, all analyzed HBD genomes encode multiple sensory receptors, except *R. palustris*, which lacks sensory receptors for aspartate and galactose (Tar and Trg). The bacterial chemotaxis system is likely to be evolutionarily fine-tuned for optimal performance [75], and it is therefore likely that HBDs have optimized their chemotaxis apparatus to respond to environmentally relevant compounds. The observation that *P. stutzeri* exhibited higher levels of chemotactic attraction toward phytoplankton-derived DOM than the rich 10% ZoBell broth used as positive control illustrates this point. Additionally, all putative HBDs included in our analysis are capable of responding to a wide array of substrates, consistent with previous reports of cultivated HBDs having genetic capacity for a high metabolic versatility [68, 69].

In support of our experimental findings, the three HBD MAGs assigned to the *Pseudomonadales* order included in our bioinformatic survey all had the genetic potential for motility and chemotaxis. *Pseudomonas* has been found associated with particles [26, 28] and the genus is prevalent, and often dominant, in diazotrophic communities from temperate estuaries and the major ocean basins [3, 4, 11, 77]. The colonization of particulate matter by *Pseudomonas*-like HBDs could therefore be an important global phenomenon.

Our survey of HBD genomes revealed that all of the examined diazotroph genomes and MAGs, except for UCYN-A, harbored an aerotaxis receptor (Aer) enabling their movement in response to oxygen gradients. It has previously been demonstrated that chemotaxis facilitated N_2 fixation by cultivating *P. stutzeri* in an oxygen gradient [45, 78]. This process requires negative aerotaxis; i.e., bacterial movement away from increasing oxygen concentration. Such negative aerotaxis has also been observed for strains of *Desulfovibrio* [71], which is consistent with the presence of the aerotaxis gene in the *Desulfovibrio* MAG (TARA-HBD01) included in our survey. Based on these previous reports and the findings of the present study, we propose that marine HBDs use aerotaxis coupled with chemotaxis to actively seek out particle-associated microenvironments with low-oxygen conditions suitable for N_2 fixation.

Raina and coauthors [42] recently addressed the importance of chemotaxis for the microscale organization of the ocean's microbiome. Here, we used a subset of that dataset [42] to show that chemotaxis toward compounds of phytoplankton origin is prevalent among marine HBDs. This was demonstrated by the motility and chemotaxis of HBDs in the field deployment but also by the finding that *P. stutzeri* was highly attracted to exudates of a stationary phase culture of *C. reinhardtii* (*Chlamydomonas* SN, Fig. 1B) resembling a natural late bloom scenario with spontaneous aggregate formation. Taken together, our results show that (1) organic solutes leaking from aggregates, such as those formed by phytoplankton cells and detritus, can attract HBDs; and (2) that this behavior is widespread among HBDs. Hence, our study offers a mechanism for HBDs to locate organic matter of phytoplankton origin; however, it remains to be addressed whether HBDs are generally enriched in functions (e.g., attachment, secretion, quorum sensing) that can mediate interactions with phytoplankton particulate matter. These functions are indeed enriched among chemotactic bacteria from natural assemblages [42]. Future experimental work using natural aggregates, single-cell methods, and rate measurements could decipher (1) whether HBDs use chemotaxis to find and colonize marine aggregates; (2) if they can or need to distinguish live and dead particulate matter; and (3) if they use aerotaxis to find low-oxygen microzones on aggregates suitable for N_2 fixation [22].

DATA AVAILABILITY

The raw FASTQ read files were deposited in the Sequence Read Archive (SRA) (accession number: PRJNA639602). The AMI MAGs used in this work are deposited on figshare (https://doi.org/10.6084/m9.figshare.13292774). We have also made publicly available (1) the metagenomic reads that mapped to *nifH* (https://doi.org/10.6084/m9.figshare.13027634), (2) the data used to generate the phylogenetic placement of metagenomic reads including *nifH* reference and environmental sequences used to construct the phylogenetic tree, collection of metagenomic reads (>100 bps), and the output from the phylogenetic placement (https://doi.org/10.6084/m9.figshare.13027706), as well as (3) seed protein alignments (https://doi.org/10.6084/m9.figshare.13027760) and (4) the custom HMMs (https://doi.org/10.6084/m9.figshare.13027781) for each of the investigated proteins included in the genetic survey of motility and chemotaxis.

REFERENCES

1. Karl D, Michaels A, Bergman B, Capone D, Carpenter E, Letelier R, et al. Dinitrogen fixation in the world's oceans. In: Boyer EW, Howarth RW, editors. The nitrogen cycle at regional to global scales. Dordrecht: Springer; 2002. p. 47–98.
2. Berthelot H, Benavides M, Moisander PH, Grosso O, Bonnet S. High-nitrogen fixation rates in the particulate and dissolved pools in the Western Tropical Pacific (Solomon and Bismarck Seas): N_2 fixation in the Western Pacific. Geophys Res Lett. 2017;44:8414–23.
3. Rahav E, Bar-Zeev E, Ohayion S, Elifantz H, Belkin N, Herut B, et al. Dinitrogen fixation in aphotic oxygenated marine environments. Front Microbiol. 2013;4:227.
4. Bentzon-Tilia M, Traving SJ, Mantikci M, Knudsen-Leerbeck H, Hansen JL, Markager S, et al. Significant N_2 fixation by heterotrophs, photoheterotrophs and heterocystous cyanobacteria in two temperate estuaries. ISME J. 2015;9:273–85.
5. Messer LF, Doubell M, Jeffries TC, Brown MV, Seymour JR. Prokaryotic and diazotrophic population dynamics within a large oligotrophic inverse estuary. Aquat Micro Ecol. 2015;74:1–15.
6. Sipler RE, Gong D, Baer SE, Sanderson MP, Roberts QN, Mulholland MR, et al. Preliminary estimates of the contribution of Arctic nitrogen fixation to the global nitrogen budget. Limnol Oceanogr Lett. 2017;2:159–66.
7. Benavides M, Bonnet S, Berman-Frank I, Riemann L. Deep into oceanic N_2 fixation. Front Mar Sci. 2018;5:1–4.
8. Mulholland MR, Bernhardt PW, Widner BN, Selden CR, Chappell PD, Clayton S, et al. High rates of N_2 fixation in temperate, Western North Atlantic coastal waters expand the realm of marine diazotrophy. Glob Biogeochem Cycles. 2019;33:826–40.
9. Zehr JP. Nitrogen fixation by marine cyanobacteria. Trends Microbiol. 2011;19:162–73.
10. Riemann L, Farnelid H, Steward G. Nitrogenase genes in non-cyanobacterial plankton: prevalence, diversity and regulation in marine waters. Aquat Micro Ecol. 2010;61:235–47.
11. Farnelid H, Andersson AF, Bertilsson S, Al-Soud WA, Hansen LH, Sørensen S, et al. Nitrogenase gene amplicons from global marine surface waters are dominated by genes of non-cyanobacteria. PLoS ONE. 2011;6:e19223.
12. Delmont TO, Quince C, Shaiber A, Esen ÖC, Lee ST, Rappé MS, et al. Nitrogen-fixing populations of Planctomycetes and Proteobacteria are abundant in surface ocean metagenomes. Nat Microbiol. 2018;3:804–13.
13. Salazar G, Paoli L, Alberti A, Huerta-Cepas J, Ruscheweyh H-J, Cuenca M, et al. Gene expression changes and community turnover differentially shape the global ocean metatranscriptome. Cell. 2019;179:1068–1083.e21.
14. Bombar D, Paerl RW, Riemann L. Marine non-cyanobacterial diazotrophs: moving beyond molecular detection. Trends Microbiol. 2016;24:916–27.
15. Moisander PH, Benavides M, Bonnet S, Berman-Frank I, White AE, Riemann L. Chasing after non-cyanobacterial nitrogen fixation in marine pelagic environments. Front Microbiol. 2017;8:1736.
16. Eady RR, Postgate JR. Nitrogenase. Nature. 1974;249:805–10.
17. Wong PP, Burris RH. Nature of oxygen inhibition of nitrogenase from azotobacter vinelandii. Proc Natl Acad Sci USA 1972;69:672–5.
18. Berman-Frank I, Quigg A, Finkel ZV, Irwin AJ, Haramaty L. Nitrogen-fixation strategies and Fe requirements in cyanobacteria. Limnol Oceanogr. 2007;52:2260–9.
19. Inomura K, Bragg J, Follows MJ. A quantitative analysis of the direct and indirect costs of nitrogen fixation: a model based on *Azotobacter vinelandii*. ISME J. 2017;11:166–75.
20. Paerl HW. Microzone formation: its role in the enhancement of aquatic N_2 fixation. Limnol Oceanogr. 1985;30:1246–52.
21. Paerl HW, Prufert LE. Oxygen-poor microzones as potential sites of microbial N_2 fixation in nitrogen-depleted aerobic marine waters. Appl Env Microbiol. 1987;53:1078–87.
22. Riemann L, Rahav E, Passow U, Grossart H-P, de Beer D, Klawonn I, et al. Planktonic aggregates as hotspots for heterotrophic diazotrophy: the plot thickens. Front Microbiol. 2022;13:1092.
23. Braun ST, Proctor LM, Zani S, Mellon MT, Zehr JP. Molecular evidence for zooplankton-associated nitrogen-fixing anaerobes based on amplification of the *nifH* gene. FEMS Microbiol Ecol. 1999;28:273–9.
24. Farnelid H, Tarangkoon W, Hansen G, Hansen PJ, Riemann L. Putative N_2-fixing heterotrophic bacteria associated with dinoflagellate–Cyanobacteria consortia in the low-nitrogen Indian Ocean. Aquat Micro Ecol. 2010;61:105–17.
25. Scavotto RE, Dziallas C, Bentzon-Tilia M, Riemann L, Moisander PH. Nitrogen-fixing bacteria associated with copepods in coastal waters of the North Atlantic Ocean: diazotroph community in association with copepods. Environ Microbiol. 2015;17:3754–65.
26. Farnelid H, Turk-Kubo K, Ploug H, Ossolinski JE, Collins JR, Van Mooy BAS, et al. Diverse diazotrophs are present on sinking particles in the North Pacific Subtropical Gyre. ISME J. 2019;13:170–82.
27. Geisler E, Bogler A, Rahav E, Bar-Zeev E. Direct detection of heterotrophic diazotrophs associated with planktonic aggregates. Sci Rep. 2019;9:1–9.
28. Pedersen JN, Bombar D, Paerl RW, Riemann L. Diazotrophs and N_2-fixation associated with particles in coastal estuarine waters. Front Microbiol. 2018;9:2759.

29. Paerl RW, Hansen TNG, Henriksen NNSE, Olesen AK, Riemann L. N_2-fixation and related O_2 constraints on model marine diazotroph *Pseudomonas stutzeri* BAL361. Aquat Micro Ecol. 2018;81:125–36.
30. Rahav E, Giannetto MJ, Bar-Zeev E. Contribution of mono and polysaccharides to heterotrophic N_2 fixation at the eastern Mediterranean coastline. Sci Rep. 2016;6:27858.
31. Chakraborty S, Andersen KH, Visser AW, Inomura K, Follows MJ, Riemann L. Quantifying nitrogen fixation by heterotrophic bacteria in sinking marine particles. Nat Commun. 2021;12:4085.
32. Stocker R, Seymour JR, Samadani A, Hunt DE, Polz MF. Rapid chemotactic response enables marine bacteria to exploit ephemeral microscale nutrient patches. Proc Natl Acad Sci USA 2008;105:4209–14.
33. Stocker R, Seymour JR. Ecology and physics of bacterial chemotaxis in the ocean. Microbiol Mol Biol Rev. 2012;76:792–812.
34. Garren M, Son K, Raina J-B, Rusconi R, Menolascina F, Shapiro OH, et al. A bacterial pathogen uses dimethylsulfoniopropionate as a cue to target heat-stressed corals. ISME J. 2014;8:999–1007.
35. Son K, Menolascina F, Stocker R. Speed-dependent chemotactic precision in marine bacteria. Proc Natl Acad Sci USA 2016;113:8624–9.
36. Brumley DR, Carrara F, Hein AM, Yawata Y, Levin SA, Stocker R. Bacteria push the limits of chemotactic precision to navigate dynamic chemical gradients. Proc Natl Acad Sci USA 2019;116:10792–7.
37. Müller-Niklas G, Stefan S, Kaltenböok E, Herndl GJ. Organic content and bacterial metabolism in amorphous aggregations of the northern Adriatic Sea. Limnol Oceanogr. 1994;39:58–68.
38. Grossart H-P, Czub G, Simon M. Algae–bacteria interactions and their effects on aggregation and organic matter flux in the sea. Environ Microbiol. 2006;8:1074–84.
39. Smith DC, Simon M, Alldredge AL, Azam F. Intense hydrolytic enzyme activity on marine aggregates and implications for rapid particle dissolution. Nature. 1992;359:139–42.
40. Kiørboe T, Ploug H, Thygesen UH. Fluid motion and solute distribution around sinking aggregates. I. Small-scale fluxes and heterogeneity of nutrients in the pelagic environment. Mar Ecol Prog Ser. 2001;211:1–13.
41. Kiørboe T, Jackson GA. Marine snow, organic solute plumes, and optimal chemosensory behavior of bacteria. Limnol Oceanogr. 2001;46:1309–18.
42. Raina J-B, Lambert BS, Parks DH, Rinke C, Siboni N, Bramucci A, et al. Chemotaxis shapes the microscale organisation of the ocean's microbiome. Nature. 2022;605:132–8.
43. Lambert BS, Raina J-B, Fernandez VI, Rinke C, Siboni N, Rubino F, et al. A microfluidics-based in situ chemotaxis assay to study the behaviour of aquatic microbial communities. Nat Microbiol. 2017;2:1344–9.
44. Clerc EE, Raina J-B, Lambert BS, Seymour J, Stocker R. In situ chemotaxis assay to examine microbial behavior in aquatic ecosystems. J Vis Exp. 2020;159:e61062.
45. Boström KH, Riemann L, Kühl M, Hagström Å. Isolation and gene quantification of heterotrophic N_2-fixing bacterioplankton in the Baltic Sea. Environ Microbiol. 2007;9:152–64.
46. Farnelid H, Harder J, Bentzon-Tilia M, Riemann L. Isolation of heterotrophic diazotrophic bacteria from estuarine surface waters: heterotrophic diazotrophs in the Baltic Sea. Environ Microbiol. 2014;16:3072–82.
47. ZoBell CE. Studies on Marine Bacteria I. The cultural requirements of heterotrophic aerobes. J Mar Res. 1941;4:41–75.
48. Alldredge AL, Gotschalk C, Passow U, Riebesell U. Mass aggregation of diatom blooms: Insights from a mesocosm study. Deep Sea Res Part II Top Stud Oceanogr. 1995;42:9–27.
49. Thornton DCO. Diatom aggregation in the sea: mechanisms and ecological implications. Eur J Phycol. 2002;37:149–61.
50. Turner J. Zooplankton fecal pellets, marine snow and sinking phytoplankton blooms. Aquat Micro Ecol. 2002;27:57–102.
51. Schnetzer A, Lampe RH, Benitez-Nelson CR, Marchetti A, Osburn CL, Tatters AO. Marine snow formation by the toxin-producing diatom, *Pseudo-nitzschia australis*. Harmful Algae. 2017;61:23–30.
52. Dittmar T, Koch B, Hertkorn N, Kattner G. A simple and efficient method for the solid-phase extraction of dissolved organic matter (SPE-DOM) from seawater. Limnol Oceanogr Methods. 2008;6:230–5.
53. Marie D, Partensky F, Jacquet S, Vaulot D. Enumeration and cell cycle analysis of natural populations of marine picoplankton by flow cytometry using the nucleic acid stain SYBR green. Appl Environ Microbiol. 1997;63:186–93.
54. Bramucci AR, Focardi A, Rinke C, Hugenholtz P, Tyson GW, Seymour JR, et al. Microvolume DNA extraction methods for microscale amplicon and metagenomic studies. ISME Commun. 2021;1:1–5.
55. Rinke C, Low S, Woodcroft BJ, Raina J-B, Skarshewski A, Le XH, et al. Validation of picogram- and femtogram-input DNA libraries for microscale metagenomics. PeerJ. 2016;4:e2486.
56. Bolger AM, Lohse M, Usadel B. Trimmomatic: a flexible trimmer for Illumina sequence data. Bioinformatics. 2014;30:2114–20.
57. Li H. Aligning sequence reads, clone sequences and assembly contigs with BWA-MEM. ArXiv13033997 Q-Bio. 2013.
58. Suzek BE, Huang H, McGarvey P, Mazumder R, Wu CH. UniRef: comprehensive and non-redundant UniProt reference clusters. Bioinformatics. 2007;23:1282–8.
59. Kanehisa M, Goto S. KEGG: Kyoto encyclopedia of genes and genomes. Nucleic Acids Res. 2000;28:27–30.
60. Buchfink B, Xie C, Huson DH. Fast and sensitive protein alignment using DIAMOND. Nat Methods. 2015;12:59–60.
61. Clarke KR, Gorley RN, Somerfield PJ, Warwick RM. Change in marine communities: an approach to statistical analysis and interpretation. 3rd ed. Plymouth: Primer-E Ltd; 2014.
62. Katoh K, Rozewicki J, Yamada KD. MAFFT online service: multiple sequence alignment, interactive sequence choice and visualization. Brief Bioinform. 2019;20:1160–6.
63. Kozlov AM, Darriba D, Flouri T, Morel B, Stamatakis A. RAxML-NG: a fast, scalable and user-friendly tool for maximum likelihood phylogenetic inference. Bioinformatics. 2019;35:4453–5.
64. Edler D, Klein J, Antonelli A, Silvestro D. raxmlGUI 2.0 beta: a graphical interface and toolkit for phylogenetic analyses using RAxML. bioRxiv. 2019. https://doi.org/10.1101/800912.
65. Barbera P, Kozlov AM, Czech L, Morel B, Darriba D, Flouri T, et al. EPA-ng: massively parallel evolutionary placement of genetic sequences. Syst Biol. 2019;68:365–9.
66. Czech L, Barbera P, Stamatakis A. Genesis and Gappa: processing, analyzing and visualizing phylogenetic (placement) data. Bioinformatics. 2020;36:3263–5.
67. Chaumeil P-A, Mussig AJ, Hugenholtz P, Parks DH. GTDB-Tk: a toolkit to classify genomes with the Genome Taxonomy Database. Bioinformatics. 2020;36:1925–7.
68. Bentzon-Tilia M, Severin I, Hansen LH, Riemann L. Genomics and ecophysiology of heterotrophic nitrogen-fixing bacteria isolated from estuarine surface water. mBio. 2015;6:e00929–15.
69. Martínez-Pérez C, Mohr W, Schwedt A, Dürschlag J, Callbeck CM, Schunck H, et al. Metabolic versatility of a novel N_2-fixing Alphaproteobacterium isolated from a marine oxygen minimum zone: novel N_2-fixer from oxygen minimum zone off Peru. Environ Microbiol. 2018;20:755–68.
70. Hyatt D, Chen G-L, LoCascio PF, Land ML, Larimer FW, Hauser LJ. Prodigal: prokaryotic gene recognition and translation initiation site identification. BMC Bioinforma. 2010;11:119.
71. Eschemann A, Kühl M, Cypionka H. Aerotaxis in *Desulfovibrio*. Environ Microbiol. 1999;1:489–94.
72. Zhu S, Kojima S, Homma M. Structure, gene regulation and environmental response of flagella in Vibrio. Front Microbiol. 2013;4:410.
73. Silva MA, Salgueiro CA. Multistep signaling in nature: a close-up of *Geobacter* chemotaxis sensing. Int J Mol Sci. 2021;22:9034.
74. Taylor BL, Zhulin IB, Johnson MS. Aerotaxis and other energy-sensing behavior in bacteria. Annu Rev Microbiol. 1999;53:103–28.
75. Colin R, Sourjik V. Emergent properties of bacterial chemotaxis pathway. Curr Opin Microbiol. 2017;39:24–33.
76. Stocker R. Marine microbes see a sea of gradients. Science. 2012;338:628–33.
77. Turk-Kubo KA, Karamchandani M, Capone DG, Zehr JP. The paradox of marine heterotrophic nitrogen fixation: abundances of heterotrophic diazotrophs do not account for nitrogen fixation rates in the Eastern Tropical South Pacific. Environ Microbiol. 2014;16:3095–114.
78. Bentzon-Tilia M, Farnelid H, Jürgens K, Riemann L. Cultivation and isolation of N_2-fixing bacteria from suboxic waters in the Baltic Sea. FEMS Microbiol Ecol. 2014;88:358–71.

ACKNOWLEDGEMENTS

The authors acknowledge the contribution of the Marine Microbes consortium and the *Tara* Oceans consortium in the generation of data used in this publication. The Marine Microbes Initiative was supported by funding from Bioplatforms Australia and the Integrated Marine Observing System (IMOS) through the Australian Government National Collaborative Research Infrastructure Strategy (NCRIS) in partnership with the Australian research community. The authors thank H. Price for assisting with the TOC analysis. We acknowledge use of computing resources at the core facility for biocomputing at the Department of Biology, University of Copenhagen.

AUTHOR CONTRIBUTIONS

SH, JBR, GWT, PH, RS, JRS, and LR designed the experiments. SH and JBR performed the experiments. JBR and DHP generated and analyzed the complete metagenomic

dataset. SH conducted the *nifH* specific analysis. The genomic survey was carried out by SH and MO. SH, JBR, JRS, and LR wrote the manuscript. All authors edited the manuscript before submission.

FUNDING

This work was supported by the Danish Council for Independent Research (6108-00013) awarded to LR and Gordon & Betty Moore Foundation Grant (GBMF3801) awarded to JRS, RS, GWT, and PH.

COMPETING INTERESTS

The authors declare no competing interests.

ADDITIONAL INFORMATION

Supplementary information The online version contains supplementary material available at https://doi.org/10.1038/s41396-022-01299-4.

Correspondence and requests for materials should be addressed to Lasse Riemann.

Reprints and permission information is available at http://www.nature.com/reprints

Publisher's note Springer Nature remains neutral with regard to jurisdictional claims in published maps and institutional affiliations.